ADVANCED FUNCTIONAL MATERIALS
www.afm-journal.de

Materials Views
www.MaterialsViews.com

Fast Switching ITO Free Electrochromic Devices

*Jacob Jensen, Markus Hösel, Inyoung Kim, Jong-Su Yu, Jeongdai Jo, and Frederik C. Krebs**

Indium-doped tin oxide free electrochromic devices are prepared by coating electrochromic polymers onto polyethylene terephthalate substrates encompassing two different silver grids as electrodes. One design comprises a flexoprinted highly conductive silver grid electrode, yielding electrochromic devices with a response time of 2 s for an optical contrast of 27%. The other design utilizes an embedded silver grid electrode whereupon response times of 0.5 s for a 30% optical contrast are realized when oxidizing the device. A commercially available conductive poly(3,4-ethylenedioxythiophene):poly(4-styrenesulfonate acid) formulation (PEDOT:PSS) is coated onto the silver grids as a charge balancing polymer, and is in this setting found to be superior to a polypyrrole previously employed in electrochromic devices. In addition, the PEDOT:PSS layer increases the conductivity in the hexagonal grid structure.

1. Introduction

The development of electrochromic devices (ECDs) has moved from laboratory conditions into pilot plants; whereby, new challenges have emerged that include avoidance of vacuum processing steps and use of simple printing, coating, and lamination methods for deposition and assembly of the devices. If these challenges are successfully addressed, polymer based electrochromic devices will be commercially attractive and competitive to existing solutions. A main obstacle is the replacement of indium-doped tin oxide (ITO) as the transparent electrode material. ITO has been widely used as electrode material in organic electronics, but due to the scarcity of indium, substituting this material for a less expensive one would significantly reduce production costs of ECDs.[1–3] Another incitement to replace ITO is the vast amount of energy used in the sputtering process employed in the production of ITO covered substrates. By avoiding such energy consuming processes, one would be able to manufacture ECDs with limited energy consumption from materials, to manufacturing and operation.

From an operational point of view, the use of ITO as electrode material in ECDs is problematic since a low concentration of charge carriers in ITO gives rise to a large sheet resistance. It has been established that the electrode resistance has a marked effect on the response time and optical contrast of an ECD,[4] and high electrode resistance leads to a non-uniform potential across the electrode (Ohmic loss), and a non-uniform current distribution in the electrolyte.[5] By using electrodes of moderate conductivity, increasing potentials are needed to achieve satisfactory response times and optical contrast, as the ionic mobility (already impeded by the semisolid gel electrolyte) partly depends on the electric field between the two electrodes. Due to several other chemical components, increasing the potential conflicts with the voltage limits, outside of which side reactions are likely to occur. These could be redox reactions of water due to moisture in the device or irreversible oxidation or reduction of the polymer films.[6–9] Such reactions can lead to reduced optical contrast, increased response times, and ultimately render the ECD non-functional.

One approach is using thin metal grids as electrode material. Such grids have been utilized as counter electrodes in inorganic based ECDs, and we have previously shown how ITO can be replaced by flexoprinting a silver based conductive hexagonal grid onto a transparent polyethylene terephthalate (PET) substrate.[5,10] Other reports show successful substitution of ITO by organic semiconductors (mostly poly(3,4-ethylenedioxythiophene), PEDOT) for fabrication of all-organic or fully printable ECDs.[11–14] Development of ITO free ECDs is an interesting academic accomplishment, as well as a major cost reducing factor, in line with our development of commercially attractive ECDs; combining flexibility, efficient production, high operational stability and good electrochromic properties. The achievements in developing ITO free electrochromic devices are shown in **Table 1**.

In this report, we show improved polymer based ECDs, comprising thin metal grid electrodes and we address several challenges;[15,16] a) Slow and uneven switching of flexoprinted silver grid based devices: by employing a hexagonal grid pattern (as opposed to a full ITO covered surface) lateral charge transport in the resulting cells produce a blooming effect within each cell. This effect is caused by differences in surface resistance, and areas in close proximity to the metal grid lines respond faster than those in the center of a hexagon. The difference in conductivity across the electrode surface cause switching of the devices in the order of 5–10 min. This is sufficient for applications such as shading or other light-management devices, but a limiting factor for other applications. b) Electrochemical decomposition of organic material: upon switching of the silver

J. Jensen, M. Hösel, Prof. F. C. Krebs
Department of Energy Conversion and Storage
Technical University of Denmark
Frederiksborgvej 399, DK-4000, Roskilde, Denmark
E-mail: frkr@dtu.dk
Dr. I. Kim, Dr. J.-S. Yu, Dr. J. Jo
Department of Printed Electronics
Korea Institute of Machinery and Materials
Daejeon, 305–343, Korea

DOI: 10.1002/adfm.201302320

Table 1. Response times for ITO free electrochromic devices.

Electrode material[a]	Primary ECP[b]	Abs$_{max}$ [nm]	ΔT	Voltage range [V]	Response time – oxidizing [s]	Response time – reducing [s]	Refs.
PEDOT:PSS	PEDOT	650	14%	0.0 to 3.0	20	16	[12]
PEDOT:PSS	PProdot-Me$_2$[c]	540	40%	–1.2 to 1.2	8[d]	8[d]	[11]
PEDOT:PSS	PEDOT	–[e]	22–35%	0.0 to 2.0	–[e]	–[e]	[13]
Flexoprinted Ag grid/PEDOT	PProdot-EtHx$_2$[f]	550	24%	–0.5 to 1.0	2	3.4	This work
Embedded Ag grid/PEDOT	PProdot-EtHx$_2$[f]	550	29%	–0.5 to 1.0	0.3	2.5	This work

[a]Material used for both electrodes; [b]ECP: Electrochromic polymer; [c]Poly((2,2-bis-methyl-propylene-1,3-dioxy)-3,4-thiophene-2,5-diyl); [d]It is unclear whether the response time given is for both redox processes; [e]Abs$_{max}$ and response time where not available. The report presented ECDs showing a range of ΔT values; [f]Poly((2,2-bis(2-ethylhexyloxymethyl)-propylene-1,3-dioxy)-3,4-thiophene-2,5-diyl).

grid based ECD, a discoloring of the device was observed, that was initially attributed to electrochemical decomposition of surfactants in the silver nanoparticle based ink used for printing the hexagonal grid structure. By using post-treated Ag-grid foils using intensive pulsed light (photonic sintering of the silver) the surfactants were satisfactorily removed,[12] but further investigation revealed that decomposition of the charge balancing polypyrrole used in the ECDs was partly responsible for the discoloration. c) Macroscopic gridlines: as the flexoprinted gridlines are currently of dimensions that cause some optical distortion when viewed at a close distance, an embedded grid having line widths of just 15 microns was explored as a less visible semi-transparent electrode grid material.

2. Results and Discussion

The two electrodes in ECDs must be able to accommodate the charge species that migrate to them during device operation in order to ensure electrochemical stability. If not protected by an electroactive species that can balance the charged species, irreversible redox reactions can occur directly on the electrode surface, with the risk of gradually lowering device performance.[21] Naturally, one electrode is coated with the primary ECP that ensures charge balance by reversible redox reactions. The other electrode should likewise by coated with an electroactive species, that ideally operate within the same potential range to ensure optimal response time and contrast.[22,23] Since most absorptive-transmissive (A/T) devices require the viewer to see through the device in the transmissive state, both electrodes need to be transparent. One way of resolving this is by using polymers that change color complementary too each other, which implies that one polymer is cathodically coloring and the other is anodically coloring. While using a color complementary polymer enhances the optical density in the colored state, the optical contrast in the ECD is lowered.[24] Another drawback using this approach is that two polymers are seldom exactly color complementary, which yields devices that has colored transmissive states.[25–27]

Instead of the color complementary approach, the secondary ECP can be an electroactive compound that has minimal absorbance in the potential region employed. Such a polymer is the recently published polypyrrole: poly(N-octadecyl-(propylene-1,3-dioxy)-3,4-pyrrole-2,5-diyl), nicknamed minimally color changing polymer (MCCP).[17,27] As the name implies MCCP lends limited absorption to the visible region and we have previously made use of this polymer as a counter polymer in ECDs, due to good solubility and processing properties that allows a wide range of coating applications.[10,20] These properties qualified MCCP to be one of the best choices as counter polymer for a grid based device. Unfortunately, we found that employing MCCP in a flexoprinted grid based device produced a slight reddish taint following repeated switches at –1 V to +1 V. By carefully taking the device apart, the discoloring was found to reside on the electrode coated with MCCP. It should be noted that we have never observed discoloring of MCCP in devices employing MCCP coated onto ITO in this potential range, and MCCP films are reported to retain 50% electroactivity (measured as current density) during 325 000 redox cycles between –0.5 V and 0.5 V for 5 s each in an argon purged electrolyte solution. In electrochromic devices, however, the chemical environment and operating conditions is different from standard laboratory test conditions. ECDs encompassing MCCP and poly((2,2-bis(2-ethylhexyloxymethyl)-propylene-1,3-dioxy)-3,4-thiophene-2,5-diyl (ECP-magenta) have been found to require potentials between –2 V and +2 V or –0.6 V and +1.4 V, depending on electrolyte composition and response time requirements.[17,20]

A second obstacle in using MCCP in combination with the silver grid electrodes is the blooming effect previously reported and shown in **Figure 1**A.[10] As the areas between the grid lines are non-conductive, the hexagonal grid structures result in an inhomogeneous electrical field between the two electrodes. This requires lateral charge transport for redox switching to occur, and the results is a slow uneven switching, as shown in Figure 1A.

2.1. Dual Functionality of PEDOT:PSS

To address the problems in using MCCP in combination with the silver grid design, a commercially available PEDOT:PSS formulation was employed as the counter polymer. PEDOT:PSS is well characterized, and polythiophenes are known to possess

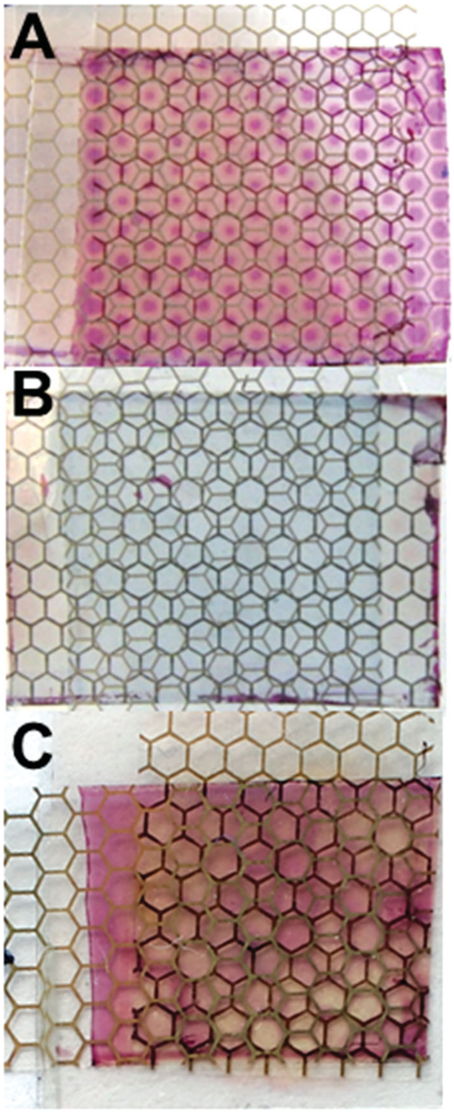

Figure 1. Flexoprinted silver grid electrodes. A) The blooming effect due to an inhomogeneous electrical field for an ECD comprising MCCP and ECP-magenta. B) ECD (in the oxidized state) where MCCP has been substituted by a conductive PEDOT:PSS formulation. The blooming effect is not observed in this device. The grid substrate has been post treated with IPL. C) ECD encompassing a flexoprinted silver grid that has not been post-treated using intensive pulsed light (IPL). This causes brown patches to form around the grid lines.

higher electrochemically stability than polypyrroles.[6,28–30] In addition to the charge balancing function, the coating of PEDOT on top of the silver grid increased the conductivity in the hexagonal grid patterns. The conductive PEDOT:PSS coating homogenized the electrical field such that the blooming effect was not observed and the devices switched evenly between the two redox states (compare Figure 1A and 1B). While both PEDOT and ECP-magenta are cathodically coloring polymers, the absorption that the thin PEDOT:PSS layer lends to the device is very limited as shown by Figure S2 in the Supporting Information. Figure S2A shows the absorption spectra (350–800 nm) for a device comprising only PEDOT:PSS on both electrodes layers switched at –0.5 V and +1.5 V, while Figure S2B shows the transmittance at 550 nm (Abs_{max}) for the same device switched between –0.5 V and 1.5 V. ΔT at 550 nm was found to be 2%.

2.2. Photonic Flash Sintering vs Non-Flashed Grid Electrodes

Figure 1B,C shows the difference in appearance after 20 switches at –1 V/+ 1.5 V between two ECDs based on flexoprinted silver-grid electrodes, with the only difference being that the grid in (B) has been post-treated using intensive pulsed light (IPL, photonic flash sintering) with a voltage setting of 3.6 kV (Sinteron 2000, Xenon Corp.) in a roll-to-roll process at 1 m min^{-1} prior to coating of polymers and electrolyte.[15] It should be noted that the silver grid was already fully sintered during the drying process while printing and the additional effect of an increased conductivity is small for the specific silver ink used here. As seen from Figure 1C, brown patches form around the grid lines that have not been post-treated. We believe the origin of this discoloring to be redox byproducts from the surfactants in the silver based ink caused by electrochemical oxidation and reduction of the device, possibly having reacted with the polymer layer coated directly on top. These byproducts are not to be seen in the devices comprising post-treated foils (Figure 1B).

2.3. Response Time

The response time partly defines the application possibilities of an electrochromic device. Since a common protocol on how to report response time have not been defined, response times are reported for a variety of ΔT values. The fastest response times are naturally linked to the smallest changes in optical contrast; however, it does make sense to report a series of response times based on different levels of optical contrast. As the majority of the redox reactions (and hence color change) occur in the beginning of a switch, 90% of a full switch might occur in two seconds while the remaining 10% of the switch takes 10 s to complete. In reporting response time, we focus on the optical contrast obtainable in relation to a given switch length rather than in relation to a percentage of a complete switch. This means that the 100% switch reported in **Figure 2** is 100% of the transmittance change achievable during a period of 10 s. In order to ease comparison with other ECDs, a full response time investigation is provided in the Supporting Information, Figure S3, which shows a full switch (maximum obtainable optical contrast) of 33% in 44 s at –0.5 V/+1.5 V. But fully switching an ECD lowers the long term stability, most likely due to electrochemically initiated side reactions. Figure 2 shows the response times for a 2 cm × 2 cm ECD based on the flexoprinted hexagonal silver grid and PEDOT:PSS coating to be 10 s for an optical contrast of 30% (550 nm) at –0.5 V and +1.5 V. Also of interest is the 26% optical contrast obtainable in approximately 2 s (depending on direction of the switch) at the same potentials, and the graph shows that a ΔT of 24% is obtainable in 10 s at –0.5 V and + 1 V.

% switch	Colour	to	Bleach	ΔT (%)	Time (s)
100	8.5		37.6	29.1	10.0
98	8.5		37.0	28.5	7.0
95	8.5		36.1	27.6	4.1
90	8.5		34.7	26.2	1.8

% switch	Bleach	to	Colour	ΔT (%)	Time (s)
100	37.6		8.5	29.1	9.5
98	37.6		9.1	28.5	6.0
95	37.6		10.0	27.6	3.8
90	37.6		11.4	26.2	2.5

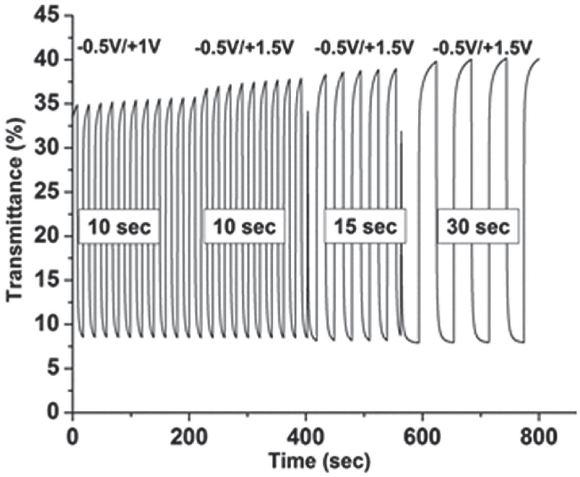

Figure 2. Response time for a 2 cm × 2 cm ECD employing a flexoprinted silver grid. The graph shows the transmittance at 550 nm for a device in response to switching at various potentials (above the graph) and switch lengths (inside the graph). The table shows the response time for the device switched between –0.5 V and +1.5 V with a switch length of 10 s.

Even though the silver grid lines in the flexoprinted silver grid are barely visible at distances beyond a few meters, a PET foil having embedded silver grid lines was employed to minimize optical distortion when the devices was viewed up close.[16,19] The line width in these foils was 15 micrometers and just noticeable as a slight blur. PEDOT:PSS coatings of a thickness similar to the flexoprinted grid devices were also employed for these devices. **Figure 3**A shows the a device employing flexoprinted Ag grid as electrodes alongside the dimensions of the gridlines, while Figure 3B shows that of a device employing embedded silver grid as electrode material. **Figure 4** shows the response times for a 1 cm × 1 cm ECD comprising the embedded silver grid. The transmittance recorded during "break in" of the device at –0.5 V/+0.5 V (the first 120 s) is included in the graph. During the break-in the optical contrast is limited to a few percent, but upon increasing the anodic potential to +1.0 V the optical contrast reaches 32%. When the potential is again lowered, the device reaches an optical contrast of 23% when switched between –0.5 V and +0.5 V. Looking at the table in Figure 4, the device generally exhibit fast response times with an optical contrast of 29% obtainable in 2.5 s when coloring and just 0.3 s when bleaching. By extending the switch to 0.8 s the optical contrast is increased to 31%, and these subsecond response times open up new possibilities for electrochromic devices. The low potentials sufficient for switching are encouraging as they serve to minimize unwanted side reactions in these devices.

2.4. Device Coloration Efficiency

The number of color centers formed as function of the charge used to evoke this change is described by the coloration efficiency, η. While high values are desirable for primary electrochromes, low values are wanted for the charge balancing polymer on the secondary electrode. Coloration efficiencies are reported in several ways, and the absence of a suitable device characteristic make comparison of devices incorporating identical polymers difficult.[31,32] Therefore, we have herein introduced the device coloration efficiency, η_d, which take the complex chemical environment of an ECD into account (compared to a standard ECP test cuvette set-up). Similar to the standard coloration efficiency, η, the device coloration efficiency η_d is given by the change in optical density at the maximum absorbing wavelength (Equation 2 divided by the charge density during that change (Equation 3). η_d is related to η by a device correction factor w, that include contributions due to electrode substrate, electrolyte matrix, and Faradaic side reactions occurring in the device (Equation 1). Knowing η_d is beneficial when designing electronic circuitry for device applications. Similar to the response time given above, η_d values are reported in relation to ΔT and not as percentages of a full switch.

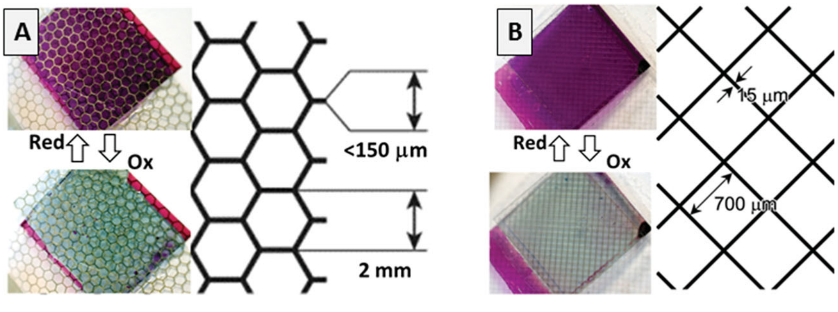

Figure 3. Dimensions of silver grid design. A) The two redox states of an ECD employing flexoprinted silver grid along a schematic showing the dimensions of the grid lines. B) A similar device, where the electrodes are from an embedded silver grid. Dimensions of the embedded grid are shown to the right.

% switch	Colour	to	Bleach	ΔT (%)	Time (s)
100	5.8		37.8	32	10
98	5.8		37.2	31.4	0.8
95	5.8		36.2	30.4	0.5
90	5.8		34.6	28.8	0.3

% switch	Bleach	to	Colour	ΔT (%)	Time (s)
100	37.8		5.8	32	10
98	37.8		6.4	31.4	6.8
95	37.8		7.4	30.4	4.4
90	37.8		9.0	28.8	2.5

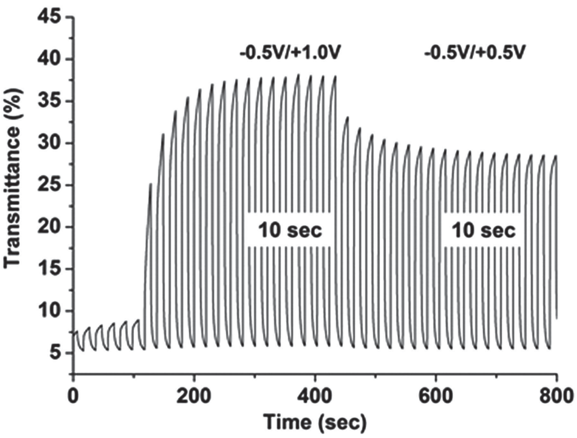

Figure 4. Response time for a 1 cm × 1 cm ECD employing an embedded silver grid. The graph shows the transmittance at 550 nm for a device in response to switching at various potentials (above the graph) for switch lengths of 10 s. The table shows the response time for the device switched between –0.5 V and +1.0 V with a switch length of 10 s.

$$\eta_d = \eta w \quad (1)$$

$$\Delta OD = \log(\%T_1/\%T_2) \quad (2)$$

$$\eta_d = (\log(\%T_1)\,\%T_2))/\,(Q_d) \quad (3)$$

Figure 5 shows η_d for a device employing ECP-magenta as the primary electrochromic polymer and flexoprinted hexagonal silver grid as transparent electrodes (solid line). The figure shows a decrease in η_d as the switch length is increased, which is to be expected as most of the color change occurs in the beginning of the switch. The most drastic change occurs during the first 10 s of the switch length where η_d drops from 310 C^{-1} cm^2 for a 1.8 s switch to 114 C^{-1} cm^2 for a 10 s switch at a potential of +1.5 V. After this the curve flattens out ending with a η_d of 20 C^{-1} cm^2 for a 60 s switch. The η_d obtained when reducing the device at –0.5 V is slightly lower for switches shorter than 10 s, but as the switch length is increased both redox reactions yield similar η_d values (additional η_d values for the two grid designs can be found in the Supporting Information, Figure S4). In devices comprising the embedded silver grid, the η_d was 391 C^{-1} cm^2 after 0.3 s, which fell to 79 C^{-1} cm^2 for a 10 s switch. For comparison, an optical contrast of 80% obtained in 0.57 s was reported for spray cast film of ECP-magenta, which gave a composite coloration efficiency of more than 1200 C^{-1} cm^2 and while such values are indeed impressive, it is worth noting they are obtained under conditions that characterize the polymer material but not devices.[18] The dashed line in Figure 5 shows the optical contrast (Δ*T*%) as a function of switch length, that is, the switch length required to reach a certain optical contrast. Since η_d and ΔT are connected by Equation 3, a decrease in η_d is observed as ΔT saturate.

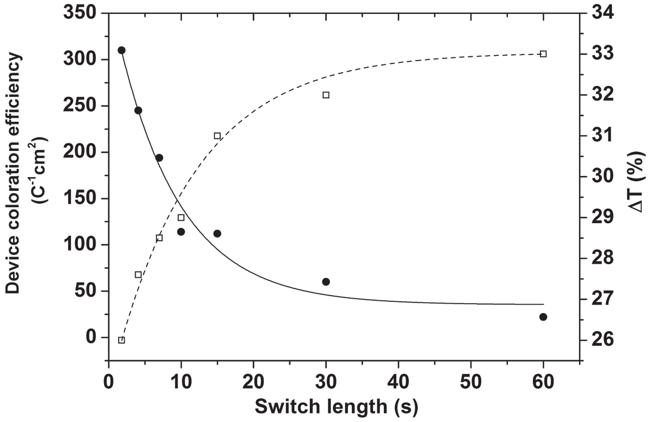

Figure 5. Device coloration efficiency as a function of switch length for an ECD employing flexoprinted silver grid as electrodes and ECP-magenta as the primary electrochromic polymer (solid line and solid circles, left *y*-axis). The dashed line shows the optical contrast as a function of switch length (open squares, right *y*-axis). Transmittance was measured at 550 nm for a device oxidized at +1.5 V. Both curves were fitted to an exponential function (R^2 values of 0.95 and 0.96).

3. Conclusion

We have shown that fast switching ITO free electrochromic devices can be manufactured on flexible substrates, by substituting ITO with a highly conducting printed silver grid as electrode material. Photonic sintering of the flexoprinted silver grid electrodes is required in order to decompose residual organic surfactants prior to coating of the electroactive polymers. PEDOT:PSS was found useful as both a stable charge balancing polymer and to increase the conductivity in the grid electrodes. By coating a conductive PEDOT:PSS formulation onto the silver grids, the electric field in the devices was homogenized and the ECDs were found to switch evenly and with appreciable speed, which is an improvement compared to previously published reports. As the length of the flexoprinted Ag web is infinite and the width is only limited by the size of the printing machine (1 m wide substrates are currently realizable, but wider substrates are not unrealistic), large area ECDs based on these substrates is certainly within reach. Flexible substrates comprising embedded silver grid electrodes were also explored and devices employing these showed better optical contrast and faster response times compared to their flexoprinted counterparts. PEDOT:PSS lowered the optical contrast of the grid based devices by 2%, which was found acceptable in comparison to the electrochemical stability induced. In perspective, this report shows that EC parameters such as response time and coloration efficiency are influenced by the setting in which they are evaluated. The standard way of characterizing EC materials can be considered a theoretical limit for a given material, while device equivalents more fully describe the practical values that can be achieved in operational devices.

4. Experimental Section

Instrumentation: Absorption/transmission spectra in the 900–300 nm range were determined using a Pharma Spec UV-1700 from Shimadzu. A Keithley 2440 Sourcemeter were used for switching the devices, and custom made software were used for logging data.

Electrochromic Polymers: poly((2,2-bis(2-ethylhexyloxymethyl)-propylene-1,3-dioxy)-3,4-thiophene-2,5-diyl) (ECP-Magenta) and poly(N-octadecyl-(propylene-1,3-dioxy)-3,4-pyrrole-2,5-diyl) (MCCP) was synthesized according to literature (with minor modifications).[17,18] The conductive PEDOT:PSS formulation was a Clevios F010 from Heraeus.

Grid Manufacture: The hexagonal grid pattern was flexo printed on a 72 μm thick PET barrier foil (Amcor) using a water-based silver ink (PChem, PFI-722) and an anilox cylinder with a volume of 3 mL m^{-2}. The printing speed was 20 m min^{-1} whereas the nanoparticle-based ink was fully dried and sintered during the printing run using IR and hot air (140 °C).[15]

For the embedded Ag grid pattern, a 15 μm line width was employed. The PET film was thermally imprinted at 110 °C using custom made machinery. The manufacturing process is described in detail elsewhere,[19] but the basic steps are summarized here: A flexible electroformed nickel-cobalt stamp holding the grid mesh is mounted on a heating roll, and heated to 200 °C. The foil is then fed through the heating roll and an impression roller during which the imprinting force and speed are 450 kgf and 0.96 m min^{-1}, respectively. Following this a water-based silver ink is filled into the engraved mesh patterns by a doctor-blade and sintered at 140 °C for 3 min. Finally residue ink is removed by a roll cleaning process.

ECD Manufacture: Prior to deposition of the ECPs the silver grid substrates was cleaned with isopropanol. The primary electrode was manufactured as follows. A PEDOT:PSS film was spincoated from a 1:2 (w:w) Clevios F010: isopropanol solution at an angular velocity of 1200 RPM. ECP-magenta (poly((2,2-bis(2-ethylhexyloxymethyl)-propylene-1,3-dioxy)-3,4-thiophene-2,5-diyl) was spincoated on top of the PEDOT:PSS layer from a 20 mg mL^{-1} toluene solution at 800 RPM. Following this a previously employed PMMA based electrolyte was spincoated at 1500 RPM.[20] The secondary electrode was manufactured as follows: A PEDOT:PSS film was spincoated from a 1:1 (w:w) Clevios F010: isopropanol solution at an angular velocity of 1000 RPM, this was followed a PMMA based electrolyte layer spincoated at 1500 RPM. Devices of 1 cm × 1 cm (embedded grid) and 2 cm × 2 cm (flexoprinted grid) were manufactured by assembling the two electrodes. A schematic depicting the layered device structure is found in the Supporting Information, Figure S1.

Supporting Information

Supporting Information is available from the Wiley Online Library or from the author.

Received: July 10, 2013
Revised: September 13, 2013

[1] European Commission, **2010**, Critical raw materials for the EU: Report of the Ad-hoc Working Group on defining critical raw materials.

[2] R. L. Moss, E. Tzimas, H. Kara, P. Willis, J. Kooroshy, **2011**, Critical Metals in Strategic Energy Technologies (JRC 65592).

[3] C. J. M. Emmott, A. Urbina, J. Nelson, *Sol. Energy Mater. Sol. Cells* **2012**, *97*, 14.

[4] H. Kaneko, K. Miyake, *Appl. Phys. Lett.* **1986**, *49*, 112.

[5] K. Ho, D. E. Singleton, C. B. Greenberg, *J. Electrochem. Soc.* **1990**, *137*, 3858.

[6] A. A. Pud, *Synth. Met.* **1994**, *66*, 1.

[7] H. Harada, T. Fuchigami, T. Nonaka, *J. Electroanal. Chem.* **1991**, *303*, 139.

[8] E. W. Tsai, S. Basak, J. P. Ruiz, J. R. Reynolds, K. Rajeshwar, *J. Electrochem. Soc.* **1989**, *136*, 3683.

[9] F. Beck, P. Braun, M. Oberst, *Ber. Bunsenges. Phys. Chem.* **1987**, *91*, 967.

[10] R. R. Søndergaard, M. Hösel, M. Jørgensen, F. C. Krebs, *J. Polym. Sci. Part B* **2013**, *51*, 132.

[11] A. A. Argun, A. Cirpan, J. R. Reynolds, *Adv. Mater.* **2003**, *15*, 1338.

[12] D. Mecerreyes, R. Marcilla, E. Ochoteco, H. Grande, J. A. Pomposo, R. Vergaz, J. M. Sánchez Pena, *Electrochim. Acta* **2004**, *49*, 3555.

[13] P. Andersson, R. Forchheimer, P. Tehrani, M. Berggren, *Adv. Funct. Mater.* **2007**, *17*, 3074.

[14] J. Kawahara, P. Andersson Ersman, D. Nilsson, K. Katoh, Y. Nakata, M. Sandberg, M. Nilsson, G. Gustafsson, M. Berggren, *J. Polym. Sci. Part B* **2013**, *51*, 265.

[15] M. Hösel, F. C. Krebs, *J. Mater. Chem.* **2012**, *22*, 15683.

[16] J.-S. Yu, I. Kim, J.-S. Kim, J. Jo, T. T. Larsen-Olsen, R. R. Søndergaard, M. Hösel, D. Angmo, M. Jørgensen, F. C. Krebs, *Nanoscale* **2012**, *4*, 6032.

[17] E. P. Knott, M. R. Craig, D. Y. Liu, J. E. Babiarz, A. L. Dyer, J. R. Reynolds, *J. Mater. Chem.* **2012**, *22*, 4953.

[18] B. D. Reeves, C. R. G. Grenier, A. A. Argun, A. Cirpan, T. D. McCarley, J. R. Reynolds, *Macromolecules* **2004**, *37*, 7559.

[19] J.-S. Yu, G. H. Jung, J. Jo, J.-S. Kim, J. W. Kim, S.-W. Kwak, J.-L. Lee, I. Kim, D. Kim, *Sol. Energy Mater. Sol. Cells* **2013**, *109*, 142.

[20] J. Jensen, H. F. Dam, J. R. Reynolds, A. L. Dyer, F. C. Krebs, *J. Polym. Sci. Part B* **2012**, *50*, 536.

[21] D. M. De Leeuw, M. M. J. Simenon, A. R. Brown, R. E. F. Einerhand, *Synth. Met.* **1997**, *87*, 53.

[22] S. Sindhu, K. Narasimha Rao, E. S. R. Gopal, *Bull. Mater. Sci.* **2008**, *31*, 15.

[23] H. C. Ko, S. Park, H. Lee, *Synth. Met.* **2004**, *143*, 31.

[24] J. Padilla, T. F. Otero, *Electrochem. Commun.* **2008**, *10*, 1.

[25] S. A. Sapp, G. A. Sotzing, J. R. Reynolds, *Chem. Mater.* **1998**, *10*, 2101.

[26] A. Kumar, D. M. Welsh, M. C. Morvant, F. Piroux, K. A. Abboud, J. R. Reynolds, *Chem. Mater.* **1998**, *10*, 896.

[27] I. Schwendeman, R. Hickman, G. Sönmez, P. Schottland, K. Zong, D. M. Welsh, J. R. Reynolds, *Chem. Mater.* **2002**, *14*, 3118.

[28] H. Yamato, M. Ohwa, W. Wernet, *J. Electroanal. Chem.* **1995**, *397*, 163.

[29] L. Groenendaal, F. Jonas, D. Freitag, H. Pielartzik, J. R. Reynolds, *Adv Mater* **2000**, *12*, 481.

[30] F. Louwet, L. Groenendaal, J. Dhaen, J. Manca, J. Van Luppen, E. Verdonck, L. Leenders, *Synth. Met.* **2003**, *135*, 115.

[31] P. M. S. Monk, R. J. Mortimer, D. R. Rosseinsky, *Electrochromism and Electrochromic Devices*, Cambridge (UK), Cambridge University Press, **2007**.

[32] C. L. Gaupp, D. M. Welsh, R. D. Rauh, J. R. Reynolds, *Chem. Mater.* **2002**, *14*, 3964.